

Isomerization of a Peptidic Fragment Studied Theoretically in Vacuum and in Explicit Water Solvent at Finite Temperature

Yves A. Mantz,[†] Helene Gerard,[‡] Radu Iftimie,[§] and Glenn J. Martyna^{*†}

IBM T. J. Watson Research Lab, Route 134 and P.O. Box 218, Yorktown Heights, New York 10598-0218,
Laboratoire de Chimie Théorique, Université Pierre et Marie Curie, Tour 22-23, 1er étage, Case 137,
4 place Jussieu, 75252 Paris, France, and Department of Chemistry, New York University,
New York, New York, 10003-6688

Received August 25, 2003; Revised Manuscript Received February 13, 2004; E-mail: martyna@us.ibm.com

N-Methylacetamide (NMA, CH₃–CO–NH–CH₃) is of interest as a model of the peptide linkage. Its behavior at points along the *cis*–*trans* isomerization pathway contributes to our understanding of the nonprolyl peptide C(O)–N bond, a ubiquitous structural proteinaceous element that can be involved in the rate-limiting steps of protein restructuring.^{1,2} In addition, measurement of the radial and angular dependence of the solvation shell structure of NMA(aq) helps elucidate the effect of water solvent on protein function and is now feasible experimentally,³ making theoretical structural studies highly relevant. Increasingly powerful computing platforms and algorithms now permit, for the first time, an ab initio computational study of NMA in a vacuum and in explicit water solvent at finite temperature to address these issues. Our methods include umbrella sampling Car–Parrinello MD⁴ and classical MD, performed for 0.2 ns and 4 ns, respectively, in both phases at 300 K using PINY_MD^{5,6} and constrained ab initio geometry optimizations with GAUSSIAN.⁷ A pictorial description of the amide group emerges that enhances our understanding of chemical bonding, and a detailed analysis of NMA(aq) provides structural data for comparison to anticipated new experiments.

The theoretical models adopted here to describe the NMA isomerization along a *preselected* pathway, i.e., the $\angle C(H_3)–C(O)–N–C(H_3)$ dihedral angle, ω , agree well at the endpoints but differ significantly in between. Both models (ab initio: DFT-BLYP,⁸ plane-wave basis set, 70-Ry cutoff, pseudopotentials, abbreviated DFT; empirical: CHARMM22⁹ or C22) yield static geometries, relative energies, and dipole moments of *trans*- and *cis*-NMA(g) in excellent agreement¹⁰ with high-level MP2 calculations performed by ourselves⁷ and by others.^{11–13} However, both the static barrier, $\Delta E_e^{DFT} \approx \Delta E_e^{MP2} \approx 1/2 \Delta E_e^{C22}$,¹⁰ and Helmholtz free-energy maxima (Figure 1) differ by several kcal/mol. Note that our barrier only provides a rough estimate of the activation free energy, because the isomerization may involve coupling to additional degrees of freedom, e.g., methyl rotation and “floppy” amide H “wagging”, but not to the extent of slightly larger molecules¹⁴ with more low-frequency modes.

The above discrepancies between the various methods near the free-energy maxima result from several factors. The barrier height under C22 is fit to an NMR measurement,⁹ and solvation enhances the barrier by 2–3 kcal/mol;¹⁵ that of DFT (and MP2) agrees to within 3 kcal/mol of other calculations.^{15,16} Additionally, the C(O)–N bond lengthens by 0.1 Å at the barrier in both DFT and MP2 descriptions of NMA(g), but it is essentially invariant under C22. Similarly, DFT and MP2 bond angles involving N, including $\angle C(O)–N–C(H_3)$ and $\angle C(O)–N–H$, are substantially distorted.

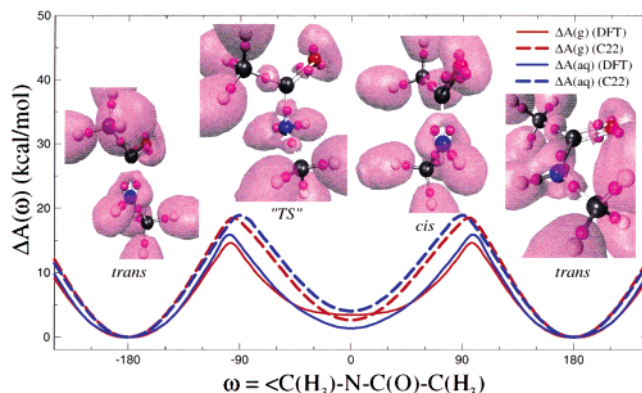


Figure 1. ELF and WFCs (see text) along with ab initio (solid line) or empirical (dashed line) predicted thermodynamic changes during isomerization. (ELF = 0.91 = purple isosurface, WFCs = small purple spheres that each carry $-2e$ charge, CPK atom colors.)

These changes indicate an underlying change in the electronic structure near/at N that bears closer examination.

Two modern tools offer a new perspective on the bonding of the amide group that adds to our understanding of this important functionality. An issue of debate is whether a charge transfer from O to N [resonance model, i.e., $C(=O)–N \leftrightarrow C(O^-)=N^+$] or from C(O) to N, Wiberg model,¹⁷ occurs when the pseudo-double C(O)–N bond in *trans*- or *cis*-NMA breaks during isomerization.¹⁸ Here, new evidence of a charge transfer from C(O) to N is offered. Wannier¹⁹ or Boys–Foster²⁰ function centers (WFCs) yield the average position of electron pairs that are depicted as (spin-paired) Lewis “dots”.²¹ The electron localization function²² (ELF) identifies spatial regions where Lewis electron-pair formation is likely, offering a check on the insights given by the WFCs. In *trans*- or *cis*-NMA, the C(O)–N bond is uniquely described by two sickle-shaped lobes (purple clouds in Figure 1) and two corresponding electron pairs (purple dots) that lie between C(O) and N in “bent” orbitals outside of the peptide plane. The “bent” orbitals can be thought of as combining an sp^2 -hybrid orbital of N with its out-of-plane p_z orbital. Although the C(O) atom is assigned five electron pairs, atomic charge neutrality is preserved based on linear interpolation of charge populations to the atom centers. During isomerization, the ELF contours and WFCs gradually evolve to an sp^2 -hybridized C(O) and sp^3 -pyramidalized N near the barrier maximum and an amine-like C(O)–N single bond, as evinced by the tetrahedral ELF lobes and WFCs; the C=O bond is relatively unchanged (Figure 1). Accordingly, the isomerization is a reactive process, because the C(O)–N “banana” bond is broken (e.g., unlike the C–C bond in butane). This analysis under DFT-BLYP offers some support for the Wiberg model, but this or any simplified

[†] IBM T. J. Watson Lab.

[‡] Université Pierre et Marie Curie.

[§] New York University.

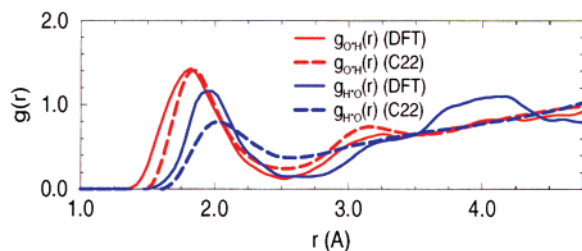


Figure 2. Solvated NMA–H₂O radial distributions.

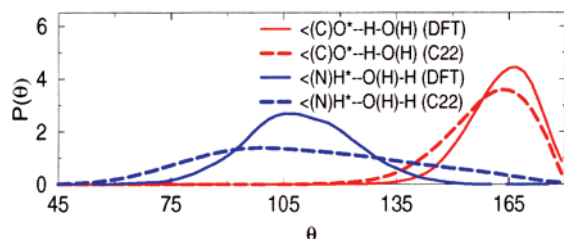


Figure 3. Solvated NMA–H₂O angular distributions.

bonding concept cannot be expected to describe all aspects of a complex many-body problem.¹⁸

Despite a 2-fold-smaller dipole moment of NMA(g) near the barrier maximum compared to *trans*- and *cis*-NMA(g) under either DFT or C22, the solvent effect on the structure and free-energy surface of NMA “dunked” in a periodic box containing 27 H₂O molecules is relatively minor in both treatments (Figure 1). The DFT barrier is increased, in accord with experiment,¹⁵ due to electronic polarization of NMA(aq); the shift in relative energy of *cis*-NMA predicted by DFT, -2.1 ± 0.5 kcal/mol, and C22, 1.4 ± 0.1 kcal/mol, models is consistent with others’ predictions.^{15,23,24} Both models agree satisfactorily with the “experimental” change in solvation free energy, $\Delta\Delta G = 0.0 \pm 0.2$ kcal/mol.²⁵ Converged results (as shown in Supporting Information) would not be expected if a reaction involving a large charge separation were modeled in such a small system. Although the solvent effect on the barrier and the solvent shell structure change, as indicated by an analysis of *trans*- and *cis*-NMA(aq) and NMA(aq) near the barrier maximum, are minor, complex coupling of solvent motions to the preselected pathway, ω , is not precluded and would be revealed by a transition path sampling calculation.²⁶

Analysis of the solvation shell reveals important differences between C22 and DFT models of NMA(aq). Select pair distribution functions and intermolecular hydrogen bond angular distributions of the carbonyl oxygen, labeled O*, and the amino hydrogen, denoted H*, interacting with H and O of water are reported for the first time in ab initio water. The C22 $g(r)$ ’s are in reasonable agreement with QM/MM simulations of *trans*-NMA(aq) by others^{24,27} and yield 2.1 H₂O neighbors hydrogen-bonded to O* and 0.9 H₂O neighbors hydrogen-bonded to H*, compared to previous results of 2.1–2.5 and 0.5–1.0, respectively.²⁷ The first peak of the DFT $g_{H^*O}(r)$ is significantly higher and narrower than the C22 result, while the DFT $g_{O^*H}(r)$ is shifted slightly to smaller values, indicating stronger hydrogen bonding (Figure 2). The DFT coordination numbers are 2.2 and 1.0, respectively.

While important, $g(r)$ ’s do not yield information regarding solvent angular distributions, a topic of great current interest.³ The angular distributions of O* and H* interacting with the nearest neighboring H₂O molecule, and the $\angle(N)-H^*\cdots O(H)-H$ distribution in particular, under DFT are narrower and shifted toward 180°

compared to C22 (Figure 3). This behavior can be explained by a preference in the directionality of hydrogen bonding within DFT resulting from the explicit inclusion of electron pairs and electronic polarization. These differences between DFT and C22 model predictions in the structure of the first solvation shell of NMA(aq) and, likely, for other species will have a substantial effect on dynamical and other static properties and merit further experimental and theoretical study.

Acknowledgment. NSF 0229959, NSERC, Drs. M. L. Klein, T. Theis, M. B. Ketchen, and J. Crain, PSC DMR020005P, IDRIS, MOLEKEL 4.3.

Supporting Information Available: An analysis of statistical errors and finite-size effects (PDF). This material is available free of charge via the Internet at <http://pubs.acs.org>.

References

- (1) Pappenberger, G.; Aygün, H.; Engels, J. W.; Reimer, U.; Fischer, G.; Kiefhaber, T. *Nat. Struct. Biol.* **2001**, *8*, 452.
- (2) Schiene-Fischer, C.; Habazettl, J.; Schmid, F. X.; Fischer, G. *Nat. Struct. Biol.* **2002**, *9*, 419.
- (3) Dixit, S.; Crain, J.; Poon, W. C. K.; Finney, J. L.; Soper, A. K. *Nature* **2002**, *416*, 829.
- (4) Car, R.; Parrinello, M. *Phys. Rev. Lett.* **1985**, *55*, 2471.
- (5) Tuckerman, M. E.; Yarne, D. A.; Samuelson, S. O.; Hughes, A. L.; Martyna, G. J. *Comput. Phys. Commun.* **2000**, *128*, 333.
- (6) Samuelson, S. O.; Martyna, G. J. *J. Chem. Phys.* **1998**, *109*, 11061.
- (7) Frisch, M. J.; Trucks, G. W.; Schlegel, H. B.; Scuseria, G. E.; Robb, M. A.; Cheeseman, J. R.; Zakrzewski, V. G.; Montgomery, J. A., Jr.; Stratmann, R. E.; Burant, J. C.; Dapprich, S.; Millam, J. M.; Daniels, A. D.; Kudin, K. N.; Strain, M. C.; Farkas, O.; Tomasi, J.; Barone, V.; Cossi, M.; Cammi, R.; Mennucci, B.; Pomelli, C.; Adamo, C.; Clifford, S.; Ochterski, J.; Petersson, G. A.; Ayala, P. Y.; Cui, Q.; Morokuma, K.; Salvador, P.; Dannenberg, J. J.; Malick, D. K.; Rabuck, A. D.; Raghavachari, K.; Foresman, J. B.; Cioslowski, J.; Ortiz, J. V.; Stefanov, B. B.; Liu, G.; Liashenko, A.; Piskorz, P.; Komaromi, I.; Gomperts, R.; Martin, R. L.; Fox, D. J.; Keith, T.; Al-Laham, M. A.; Peng, C. Y.; Nanayakkara, A.; Gonzalez, C.; Challacombe, M.; Gill, P. M. W.; Johnson, B. G.; Chen, W.; Wong, M. W.; Andres, J. L.; Head-Gordon, M.; Replogle, E. S.; Pople, J. A. *Gaussian 98*, revision A.11; Gaussian, Inc.: Pittsburgh, PA, 2001.
- (8) (a) Becke, A. D. *Phys. Rev. A* **1988**, *38*, 3098. (b) Lee, C.; Yang, W.; Parr, R. G. *Phys. Rev. B* **1988**, *37*, 785.
- (9) MacKerell, A. D., Jr.; Bashford, D.; Bellott, R. L.; Dunbrack, R. L., Jr.; Evanseck, J. D.; Field, M. J.; Fischer, S.; Gao, J.; Guo, H.; Ha, S.; Joseph-McCarthy, D.; Kuchnir, L.; Kuczyka, K.; Lau, F. T. K.; Mattos, C.; Michnick, S.; Ngo, T.; Nguyen, D. T.; Prodhom, B.; Reiher, W. E., III; Roux, B.; Schlenkerich, M.; Smith, J. C.; Stote, R.; Straub, J.; Watanabe, M.; Wiórkiewicz-Kuczera, J.; Yin, D.; Karplus, M. *J. Phys. Chem. B* **1998**, *102*, 3586.
- (10) Bonds, ± 0.03 Å; bends, $\pm 3^\circ$; *t*-, *c*-dipole (D)/ ΔE_e^{-t} , ΔE_e^{TS-t} (kcal/mol): 3.9, 4.2/2.4, 12.6 (DFT), 4.2, 4.6/2.3, 13.4 (MP2/6-311+G**), 4.1, 4.1/1.8, 20.4 (C22).
- (11) Cuevas, G.; Renugopalakrishnan, V.; Madrid, G.; Hagler, A. T. *Phys. Chem. Chem. Phys.* **2002**, *4*, 1490.
- (12) Kang, Y. K. *J. Mol. Struct. (THEOCHEM)* **2001**, *546*, 183.
- (13) Martínez, A. G.; Vilar, E. T.; Fraile, A. G.; Martínez-Ruiz, P. *J. Phys. Chem. A* **2002**, *106*, 4942.
- (14) Bolhuis, P. G.; Dellago, C.; Chandler, D. *Proc. Natl. Acad. Sci. U.S.A.* **2000**, *97*, 5877.
- (15) Luque, F. J.; Orozco, M. *J. Org. Chem.* **1993**, *58*, 6397.
- (16) Langley, C. H.; Allinger, N. L. *J. Phys. Chem. A* **2002**, *106*, 5638.
- (17) Wiberg, K. B.; Laidig, K. E. *J. Am. Chem. Soc.* **1987**, *109*, 5935.
- (18) For example, see: (a) Fogarasi, G.; Szalay, P. G. *J. Phys. Chem. A* **1997**, *101*, 1400. (b) Basch, H.; Hoz, S. *Chem. Phys. Lett.* **1998**, *294*, 117. (c) Quiñonero, D.; Frontera, A.; Capó, M.; Ballester, P.; Suñer, G. A.; Garau, C.; Deyá, P. M. *New J. Chem.* **2001**, *25*, 259. (d) Mo, Y.; Schleyer, P. v. R.; Wu, W.; Lin, M.; Zhang, Q.; Gao, J. *J. Phys. Chem. A* **2003**, *107*, 10011.
- (19) Wannier, G. H. *Phys. Rev.* **1937**, *52*, 191.
- (20) Foster, J. M.; Boys, S. F. *Rev. Mod. Phys.* **1960**, *32*, 300.
- (21) Ifimie, R.; Thomas, J. W.; Tuckerman, M. E. *J. Chem. Phys.* **2004**, *120*, 2169.
- (22) Becke, A. D.; Edgecombe, K. E. *J. Chem. Phys.* **1990**, *92*, 5397.
- (23) Jorgensen, W. L.; Gao, J. *J. Am. Chem. Soc.* **1988**, *110*, 4212.
- (24) Yu, H.-A.; Karplus, M.; Pettitt, B. M. *J. Am. Chem. Soc.* **1991**, *113*, 2425.
- (25) Rick, S. W.; Berne, B. E. *J. Am. Chem. Soc.* **1996**, *118*, 672.
- (26) McCormick, T. A.; Chandler, D. *J. Phys. Chem. B* **2003**, *107*, 2796.
- (27) Gao, J.; Freindorf, M. *J. Phys. Chem. A* **1997**, *97*, 3182.

JA0305120